# Integrated Camera-Based Navigation

Brita Helene Hafskjold

(*Centre for Technology at Kjeller* (*UniK*))

Bjørn Jalving, Per Espen Hagen and Kenneth Gade

(*Norwegian Defence Research Establishment* (*FFI*))

This paper presents an integrated INS (Inertial Navigation System) and camera-based navigation system. The camera-based navigation system provides position measurement aiding to the INS. This is an alternative to the more conventional GPS (Global Positioning System) aided INS. The system is intended for UAVs (Unmanned Aerial Vehicles) and long-range missiles. The basic principles of camera-based navigation are presented. The Kalman filter based integration of INS and camera-based navigation is discussed. Total system simulation results are shown together with INS simulations for comparison. Finally, a brief overview of factors that improve the navigation accuracy is presented.

KEY WORDS

1. Integration. 2. Inertial Navigation. 3. Imagery.

1. INTRODUCTION. GPS is vulnerable to jamming and other disturbances. Camera-based navigation cannot be disturbed as easily, and an INS is impossible to jam. By combining camera-based navigation and INS in an integrated system, we obtain a capability that unites:

(a) the precise measurement of high frequency motion that the INS delivers, and
(b) the low position drift rate that the camera-based navigation offers.

The system contains three types of sensors:

(i) A camera (strapdown), capturing the terrain. The raw image data are fed into an image-processing algorithm, the output of which is a set of recognisable points in the image. Camera-based navigation is described in more detail in Section 3.
(ii) An IMU (Inertial Measurement Unit) containing three gyroscopes and three accelerometers.
(iii) An altimeter (e.g. an air pressure transmitter).

An existing digital elevation map is also used.

This work is based on the camera-based navigation research found in Hagen (1993) and the INS work in Gade (1997). The contribution of this research is the integration of these two systems. Two textbooks on INS that can be recommended are Britting (1971) and Titterton & Weston (1997).

2. MATHEMATICAL NOTATION. The mathematical notation used in this paper is:

| | | | |
|---|---|---|---|
| $p$ | image token | $I$ | inertial coordinate system |
| $l$ | landmark | $L$ | local coordinate system |
| $\hat{x}$ | estimate of $x$ | $C$ | camera coordinate system |
| $\tilde{x}$ | measurement of $x$ | $B$ | body coordinate system |
| $x_k$ | value of $x$ at time $k$ | $E$ | earth coordinate system |
| $x^A$ | vector $x$ decomposed in coordinate system $A$ | $P$ | picture coordinate system |
| | | $M$ | map coordinate system |

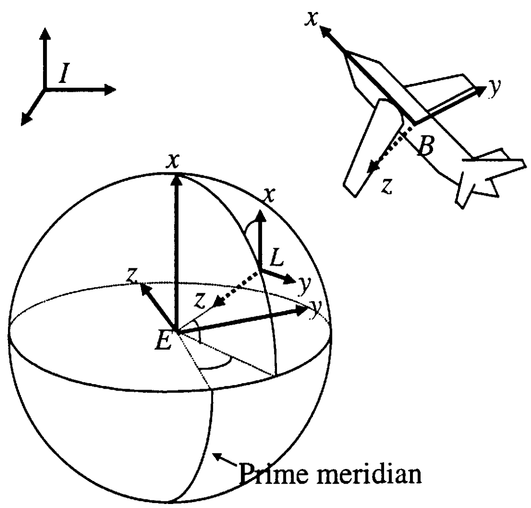


Figure 1. Coordinate systems B, I, E and L.

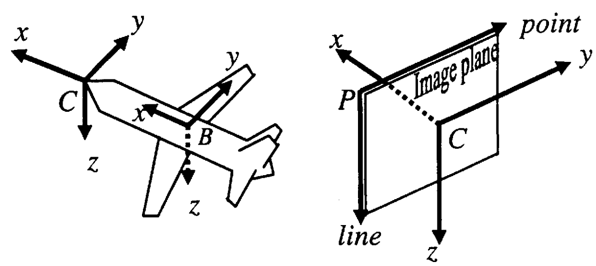


Figure 2. Coordinate systems B, C and P.

The coordinate systems used in this paper are depicted in Figures 1 and 2. $M$ is a local level coordinate system, similar to $L$ but fixed to the earth.

3. PRINCIPLES OF CAMERA-BASED NAVIGATION. Camera-based navigation has traditionally been used to navigate across a pre-mapped terrain, which means that a flight must be performed over the specified route to gather either easy-to-recognise structures in the picture or whole pictures. During subsequent flights, the camera pictures are compared to these stored pictures, and the position and attitude of the vehicle can be calculated.

The system described in this paper does not require pre-mapping. The easy-to-recognise objects must be chosen, and their ground position determined, during each flight. This is done by the image processing routine, which chooses an *image token* as a point in the image that will be easy to recognise in the next image in the sequence. The movements of these *image tokens* in the subsequent images provide information about the topography of the depicted landscape (and the vehicle movement). The use of this information, which is dependent on the position of the camera relative to the terrain, together with an elevation map, provides a method that is quite different from the traditional 'optical flow' algorithm. The image processing routine is fully explained in Hagen (1993). A *landmark* is a point on the terrain surface that corresponds to an image token. In the system, INS position and attitude are used to calculate the landmark position, as illustrated in Figure 3.

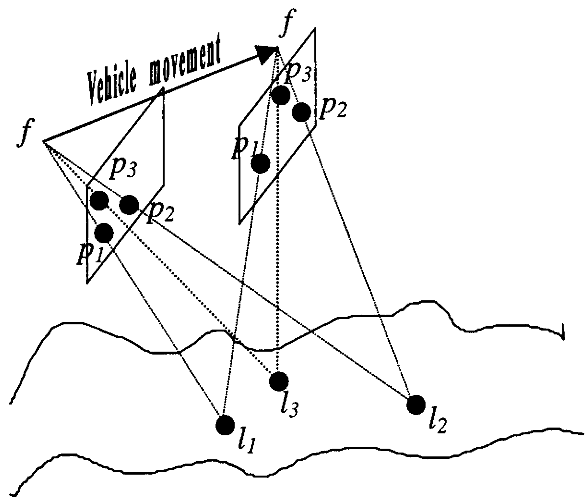


Figure 3. Principles of the camera-based navigation system. ($f$ = focal point of the camera, $p_i$ = *image token i*, $l_i$ = *landmark i*.)

The image tokens will remain in the image as long as the corresponding landmarks are in the line-of-sight of the camera; that is, within the camera aperture angle. When an image token disappears from the image, a new landmark must be chosen. Image tokens can also be lost because of changes in perspective, where a landmark can be hidden behind a hill, the scene changes (such as cars driving down a road), or due to mist or other circumstances that render the image tokens unrecognisable in the next image. Because a constant number of landmarks is preferred, a new landmark is chosen each time an image token is lost. This is conducted by the image processing routine, as described above.

## 4. INTEGRATION OF INS AND CAMERA-BASED NAVIGATION.

The integrated system works as follows. At each time iteration, the INS computes an estimate of the vehicle position and attitude. The integration with the camera-based navigation is carried out by using these estimates together with the position of the landmarks to calculate predicted positions of the image tokens. The difference between these predicted positions and the measured positions of the image tokens is

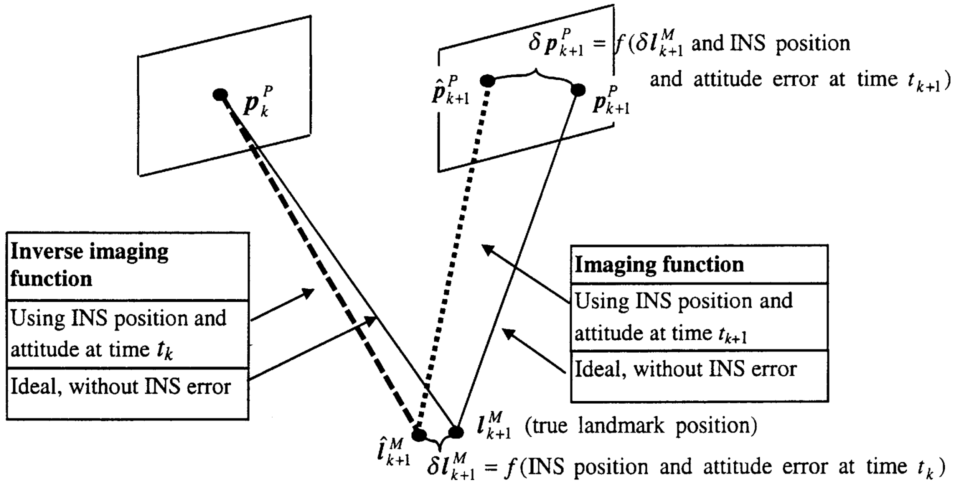


Figure 4. The difference between the calculated ($\hat{p}_{k+1}^P$) and the true ($p_{k+1}^P$) image token position, $\delta p_{k+1}^P$, is a function of the INS error. $l_{k+1}^M$ is the true and $\hat{l}_{k+1}^M$ is the calculated landmark position given in the map co-ordinate system.

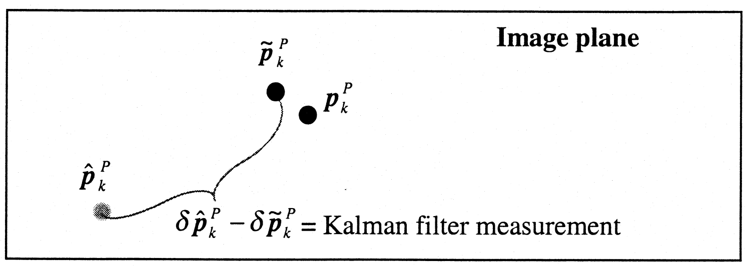


Figure 5. The difference between the calculated ($\hat{p}_k^P$) and the measured ($\tilde{p}_k^P$) image token position is used as the Kalman filter measurement.

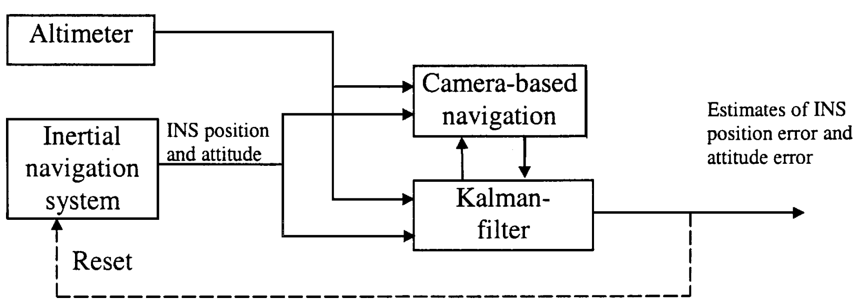


Figure 6. Total system structure.

used by an error-state Kalman filter to estimate the INS errors, as illustrated in Figures 4 and 5.

Figure 6 shows the total system structure. The camera-based navigation uses the measurements from the INS and the altimeter to calculate the image token positions in the next image, as illustrated in Figure 4.

Figure 7 shows a more detailed picture of the total structure. The box on the right

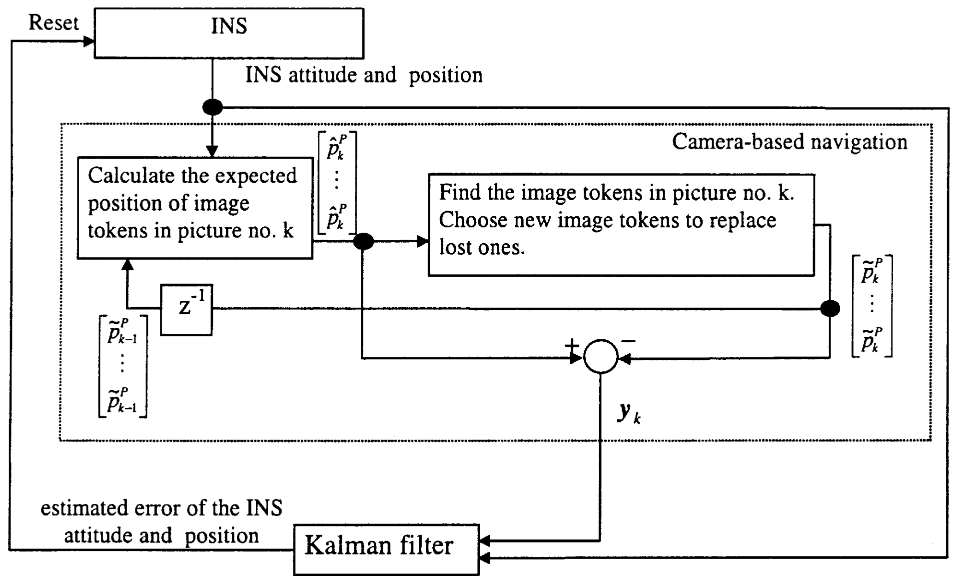


Figure 7. Main algorithm of the camera-based navigation. $\hat{\boldsymbol{p}}_k^P$ is the calculated and $\tilde{\boldsymbol{p}}_{k+1}^M$ is the measured image token position.

Table 1. IMU quality.

| Gyroscopes | | Accelerometers | |
|---|---|---|---|
| Misalignment error | 0·1 mrad ($1\sigma$) | Misalignment error | 0·1 mrad ($1\sigma$) |
| Scale factor error | 50 ppm ($1\sigma$) | Scale factor error | 100 ppm ($1\sigma$) |
| Bias error | 1°/h ($1\sigma$) | Bias error | 1 mg ($1\sigma$) |
| Angular random walk | 0·1°/$\sqrt{\text{h}}$ | Velocity random walk | Negligible |

represents the image processing routine (explained in Hagen (1993)), which measures the position of the image tokens in the next image. The Kalman filter uses the INS attitude and position estimates in its system matrix. The filter's estimate of the INS attitude and position error is used to reset the INS for each new image in the video stream.

5. SIMULATION RESULTS. The total system has been simulated with the IMU quality, terrain and trajectory given in Section 5.1. Section 5.2. shows the INS drift (corresponding to the IMU quality in Table 1) and two simulations are shown and briefly discussed in Section 5.3. A description of system behaviour is given in Section 5.4.

5.1. *Simulation Assumptions.* We have made no assumptions as to the type of aerial vehicle used in our simulations. Because the system uses the navigation equations for the IMU/INS, the only vehicle parameters included are speed, position and attitude.

5.1.1. *IMU Quality.* Table 1 shows the expected errors of the IMU used in the simulations; these represent relatively low quality system with overall error growth of $> 10$ nm per hour.

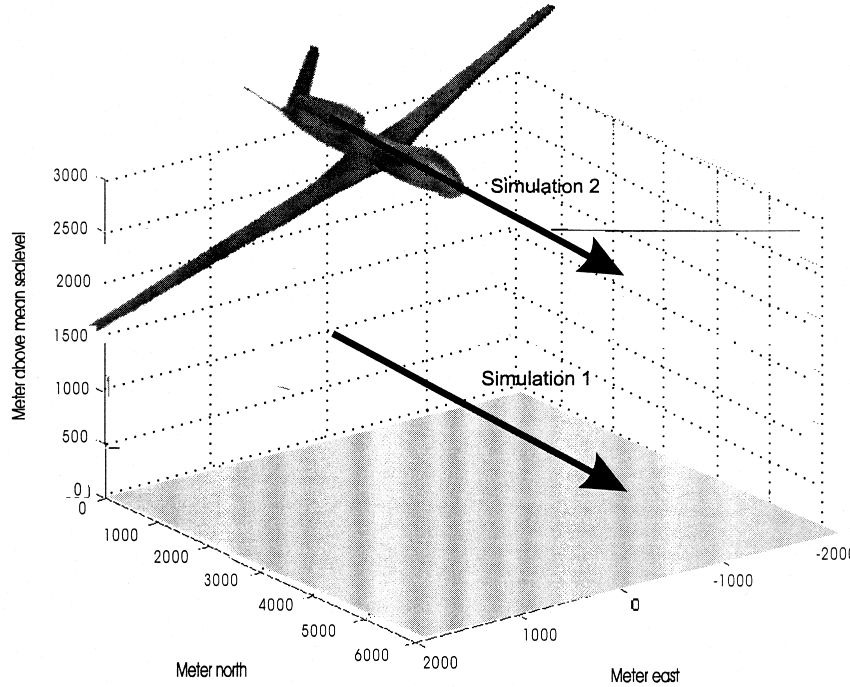


Figure 8. Simulation trajectories.

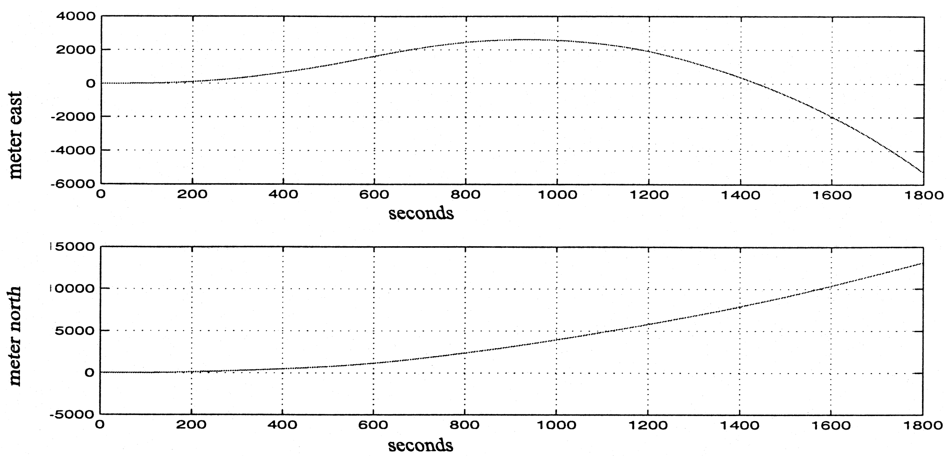


Figure 9. INS positioning error.

5.1.2. *Terrain and Trajectory.* Figure 8 shows the terrain (flat) and trajectories used in the simulations in this paper. The UAV starts out at the intersection between the prime meridian and equator, flying straight north with a speed of 50 metres per second. The vehicle height is 1000 metres above mean sea level in simulation 1 and 3000 metres above mean sea level in simulation 2.

5.2. *INS drift.* Figure 9 shows a simulation of the free inertial performance of the INS. The simulation is performed with the IMU quality and trajectory as described in Section 5.1.

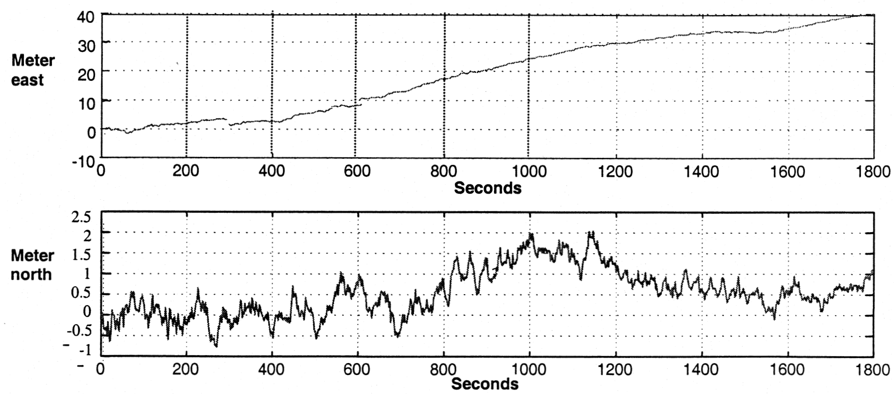


Figure 10. Total system position error of simulation 1.

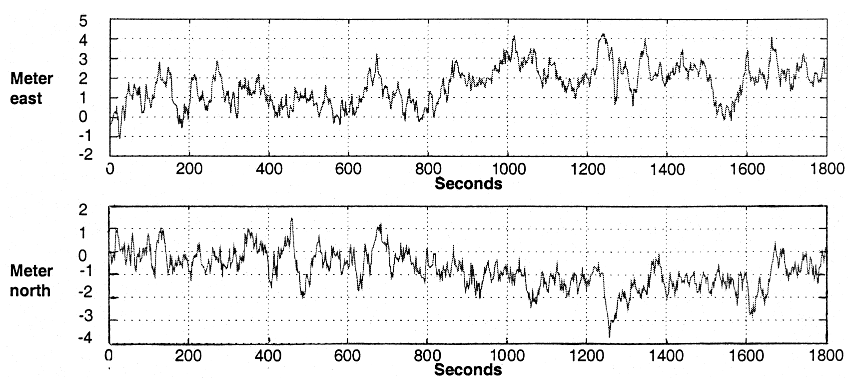


Figure 11. Total system position error of simulation 2.

5.3. *Total System Accuracy*. In this section, the simulations use the same IMU quality and trajectory as in Section 5.2., but the INS is now aided by camera-based navigation. The total system accuracy depends on numerous parameters. In order to illustrate the influence of such parameters on the total system behaviour, only one parameter, namely the vehicle height above the terrain, is changed from simulation 1 to simulation 2. The rest of the main simulation parameters are:

Picture frequency: 25 Hz
Picture size: $500 \times 500$ pixels
Camera aperture angle: 136°
Camera mounting: Downward, such that the $x$ axis of coordinate system $C$ and the $z$ axis of coordinate system $B$ are parallel.

Measurement noise: 0·8 pixels
Altimeter error std. deviation: 1 m
Number of landmarks: 12

The influence on the total system behaviour of altering these parameters is briefly discussed in Section 5.4.

Figure 10 shows simulation 1, where the vehicle height is 1000 metres above mean sea level.

Simulation 2, where the vehicle height is 3000 metres above mean sea level, is shown in Figure 11.

Figure 11 shows improved position accuracy compared to Figure 10. Increasing the distance between the vehicle and the terrain increases the time that each landmark is present in the picture. With a constant picture frequency, this gives more measurements of each landmark before it is lost.

Both simulations show more drift in the cross-track direction (east) than in the along-track direction (north). The heading uncertainty is normally the main drift source, giving drift of first order across the trajectory, and of second order along the trajectory.

5.4. *System Behaviour*. Increasing the picture frequency provides more measurements of each landmark before its corresponding image token is lost (that is, before it is out of sight of the camera). With all other parameters unchanged, this reduces the influence of the measurement noise, thereby increasing the navigation accuracy.

Increasing the number of pixels in the image increases the picture resolution, thereby decreasing the measurement noise.

Enlarging the camera aperture angle increases the time that each image token is present in the picture, thereby allowing more measurements of each landmark, which should improve the total system accuracy. However, increasing the camera aperture angle, results in a wider angle covered by each pixel, so that the measurement noise (in pixels) corresponds to a larger area on the ground, which decreases the total system accuracy.

Changing the camera orientation from pointing straight downward to 45° forward reduces the system drift. This increases the time that each landmark is in the line-of-sight of the camera, contributing to an increased number of measurements of each landmark.

Undulating terrain beneath the vehicle improves the geometrical distribution of the landmarks, making it easier to solve ambiguities such as roll versus position in the cross-track direction and pitch versus position in the along-track direction. Simulations in Hafskjold (1999) show that this improves camera-based navigation performance.

## 6. CONCLUSIONS.

This paper has discussed a method for aiding an INS with a camera-based navigation system, and the effect of system parameters on navigation performance. Hafskjold (1999) showed that the total system accuracy can be improved by:

(i) Increased picture frequency.
(ii) Increased number of landmarks (this requires more computing power, since each new landmark adds 3 elements to the Kalman filter state vector).
(iii) Decreased picture measurement noise (for example, by avoiding areas covered in mist or smoke, decreasing the camera aperture angle or increasing the picture resolution by increasing the number of pixels in the image).
(iv) Increased time in which each image token is present in the image (for example, by reducing the vehicle speed, increasing the vehicle height above the terrain or increasing the camera aperture angle).
(v) Increased geometrical distribution of the landmarks (for example, by choosing undulating terrain or by reducing the vehicle height above the terrain).

The INS in the simulations has been of the $> 10$ nm per hour class, which is usually found in missiles, UAVs etc. Military and civilian aeroplanes are normally equipped with the more accurate 1 nm per hour type of systems. Using a more accurate INS will give higher accuracy or alternatively put less demand on the camera-based navigation system aiding.

## REFERENCES

Hagen, P. E. (1993). Navigation by images. *Modelling*, *Identification and Control*, Vol. 14, No.3.

Gade, K. (1997). *Integrering av treghetsnavigasjon i en autonom undervannsfarkost* (in Norwegian). Institutt for teknisk kybernetikk, Norwegian University of Science and Technology.

Britting, K. R. (1971). *Inertial Navigation Systems Analysis*. Wiley Interscience.

Titterton, D. H. and Weston, J. L. (1997). *Strapdown Inertial Navigation Technology*. Peter Peregrinus Ltd, Herts, U.K.

Hafskjold, B. H. (1999). *Integrert bildebasert navigasjon* (in Norwegian). FFI/Rapport-99/02703, Norwegian Defence Research Establishment.